

Co-delivery of novel bispecific and trispecific engagers by an amplicon vector augments the therapeutic effect of an HSV-based oncolytic virotherapy

Divya Ravirala,¹ Brandon Mistretta,^{1,2} Preethi H Gunaratne,^{1,2} Guangsheng Pei ,³ Zhongming Zhao ,³ Xiaoliu Zhang ¹

To cite: Ravirala D, Mistretta B, Gunaratne PH, *et al.* Co-delivery of novel bispecific and trispecific engagers by an amplicon vector augments the therapeutic effect of an HSV-based oncolytic virotherapy. *Journal for ImmunoTherapy of Cancer* 2021;9:e002454. doi:10.1136/jitc-2021-002454

► Additional online supplemental material is published online only. To view, please visit the journal online (<http://dx.doi.org/10.1136/jitc-2021-002454>).

Accepted 16 May 2021



© Author(s) (or their employer(s)) 2021. Re-use permitted under CC BY-NC. No commercial re-use. See rights and permissions. Published by BMJ.

¹Center for Nuclear Receptors and Cell Signaling, Department of Biology and Biochemistry, University of Houston, Houston, Texas, USA

²UH Seq-N-Edit Core, Department of Biology and Biochemistry, University of Houston, Houston, Texas, USA

³Center for Precision Health, School of Biomedical Informatics, The University of Texas Health Science Center at Houston, Houston, Texas, USA

Correspondence to
Dr Xiaoliu Zhang;
shaunzhang@uh.edu

ABSTRACT

Background Although oncolytic virotherapy has shown substantial promises as a new treatment modality for many malignancies, further improvement on its therapeutic efficacy will likely bring more clinical benefits. One plausible way of enhancing the therapeutic effect of virotherapy is to enable it with the ability to concurrently engage the infiltrating immune cells to provide additional antitumor mechanisms. Here, we report the construction and evaluation of two novel chimeric molecules (bispecific chimeric engager proteins, BiCEP and trispecific chimeric engager protein, TriCEP) that can engage both natural killer (NK) and T cells with tumor cells for enhanced antitumor activities.

Methods BiCEP was constructed by linking orthopoxvirus major histocompatibility complex class I-like protein, which can selectively bind to NKG2D with a high affinity to a mutant form of epidermal growth factor (EGF) that can strongly bind to EGF receptor. TriCEP is similarly constructed except that it also contains a modified form of interleukin-2 that can only function as a tethered form. As NKG2D is expressed on both NK and CD8⁺ T cells, both of which can thus be engaged by BiCEP and TriCEP.

Results Both BiCEP and TriCEP showed the ability to engage NK and T cells to kill tumor cells *in vitro*. Coadministration of BiCEP and TriCEP with an oncolytic herpes simplex virus enhanced the overall antitumor effect. Furthermore, single-cell RNA sequencing analysis revealed that TriCEP not only engaged NK and T cells to kill tumor cells, it also promotes the infiltration and activation of these important immune cells.

Conclusions These novel chimeric molecules exploit the ability of the oncolytic virotherapy in altering the tumor microenvironment with increased infiltration of important immune cells such as NK and T cells for cancer immunotherapy. The ability of BiCEP and TriCEP to engage both NK and T cells makes them an ideal choice for arming an oncolytic virotherapy.

INTRODUCTION

The intrinsic propensity of the oncolytic viruses (OVs) to selectively infect, replicate in, and kill malignant cells makes them attractive candidates as emerging anticancer agents. Considerable progress has been made

in recent years on oncolytic virotherapy research, which has led to preclinical and clinical evaluation of a range of OVs, including those derived from herpes simplex virus (HSV),¹ vesicular stomatitis virus,² adenovirus,³ vaccinia virus,⁴ and measles virus.⁵ Talimogene laherparepvec (T-VEC or Imlygic) is a genetically modified type I HSV (HSV-1) and is the first and only OV therapy to be approved for the treatment of advanced melanoma by the US FDA (US Food and Drug Administration).⁶ However, despite these exciting developments, it is noticeable that T-VEC has manifested only moderate benefits in patients with advanced melanoma. Thus, there is a need to further improve the efficacy of oncolytic virotherapy. One plausible way of achieving this is to combine virotherapy with other common therapeutic strategies, particularly with immunotherapy.⁷ Indeed, recent clinical studies have shown that the therapeutic effect can be significantly improved by combining virotherapy with checkpoint inhibitors.⁸ Oncolytic virotherapy interacts with the host's immunity in many ways, and a full understanding of these interactions will likely lead to the design of new strategies for synergizing viroimmunotherapy.

One way that OVs interact with the host's immune system is to induce immunogenic death of tumor cells by releasing abundant tumor-associated antigens (TAA's) and neoantigens, as well as pathogen-associated molecular patterns and damage-associated molecular pathogens.⁹ Additionally, viral infection induces local inflammation, which can stimulate dendritic cell (DC) maturation. Mature DCs then migrate to the draining lymph nodes where they present the tumor antigens to the T cells, and the activated CD4⁺ and CD8⁺ effector T cells can potentially kill both infected and uninfected tumor cells.¹⁰



To enhance the antitumor immune responses, OV_s have been armed with a variety of immunostimulatory genes. For example, GM-CSF has been inserted into several OV_s, including HSV-1-based T-VEC, adenovirus-based CG0070, Vaccinia virus-based JX-594.¹¹

Studies in recent years from us and others have shown that virotherapy can also impact the immune cell landscape by attracting the migration of immune cells to tumor microenvironment (TME),^{12–13} the so-called converting ‘cold tumors’ to hot ones. Other studies have shown that there is an early influx of innate immune cells, including macrophages and natural killer (NK) cells, in response to tumor virotherapy. Several strategies have been developed to exploit the changes in the immune landscape during virotherapy by converting the infiltrating immune cells to attack tumor cells. For example, it was reported that arming an oncolytic vaccinia virus with a secretory bispecific T-cell engager (BiTE) consisting of two single-chain variable fragments (scFvs) specific for CD3 and the tumor cell surface antigen EphA2 can significantly enhance antitumor therapy.¹⁴ BiTE has since been incorporated into other OV_s such as adenovirus and measles virus.^{15–16} Our recent studies show that arming an oncolytic HSV with a novel chimeric molecule that can engage NK cells with tumor cells via Protein L and a TAA ligand can also enhance the antitumor efficacy of the virotherapy.¹⁷

Here, we report a novel strategy to engage both the infiltrating T cells and NK cells in TME to kill tumor cells during virotherapy. The molecule on immune cells that we chose to engage is NKG2D, an activating receptor that is abundantly expressed on human NK and CD8⁺ T cells, murine NK cells and activated murine CD8⁺ T cells.^{18–19} In addition to engaging both NK and T cells, choosing NKG2D over the traditional CD3 allows the engagement of mainly CD8⁺ subpopulation of T cells. On the other hand, the TAA that we chose to engage is epidermal growth factor receptor (EGFR) that is overexpressed on many solid tumors.²⁰ Instead of using the traditional antibodies scFvs, we chose to use ligands as the targeting moieties. The reason for such a design is the concern on the high binding affinity of scFvs used in either BiTE or CAR-T cells and its potential link to the enhanced release of cytokines and the consequential cytokine storms.²¹ The affinity of ligand binding is usually significantly lower than that of a scFv. As such, this design mimics ‘affinity tuning’ that has been applied for increasing the safety of BiTE.²² For engaging the NKG2D molecule, we chose to use orthopoxvirus major histocompatibility complex class I-like protein (OMCP), which is a small polypeptide encoded by monkeypox and cowpox virus that can selectively bind to NKG2D with an affinity equal to, or greater than, all other known NKG2D ligands.²³ For engaging EGFR, we chose to use a mutant form of EGF (m123) that has an enhanced binding affinity and dynamic to both murine and human EGFR.²⁴ Another advantage of the design of this unique chimeric molecule is that it can be used for evaluating both human and murine immune settings. We constructed this chimeric molecule in two

different forms. A bispecific chimeric engager proteins (BiCEP) is composed of OMCP at its N-terminus and EGF (m123) at the C-terminus with a flexible linker between these two components. A trispecific chimeric engager protein (TriCEP) was constructed by incorporating a mutated interleukin 2 (IL-2) to the N-terminus of BiCEP so that it may bind to the IL-2 receptor on the engaged NK or T cells to potentiate their proliferation and functionality. Both BiCEP and TriCEP showed the capability of engaging NK or T cells to kill tumor cells when evaluated in vitro. When codelivered together with an HSV-based OV in vivo, they enhanced the antitumor therapeutic activity. Furthermore, our single-cell RNA sequence (scRNA-seq) data indicate that codelivery of these chimeric molecules can dramatically change the immune cell landscape within TME, as evidenced by increased infiltration of NK/T cells. Together, our data suggest that coadministration of these uniquely designed chimeric engagers represents a viable way of potentiating virotherapy for solid tumors.

RESULTS

Design of a novel engager that can engage both infiltrating NK cells and CD8⁺ T cells to enhance the antitumor effect of an HSV-based OV

Previous studies from us and others have shown that chimeric molecules that engage either T cells (mostly via a scFv to CD3) or NK cells can enhance the therapeutic effect of an oncolytic virotherapy.^{14–17} Here, we report the design of a novel chimeric molecule that can engage both NK and T cells. As depicted in [figure 1A](#), the key components of this chimeric molecule are at the N-terminus is a 152 amino acid OMCP and at the C-terminus is a mutant form of EGF (m123). OMCP is a small polypeptide encoded by monkeypox and cowpox virus that can selectively bind to NKG2D with an affinity equal to, or greater than, all other known NKG2D ligands.²³ The mutated EGF α ligand (EGFm123) has an enhanced binding affinity and dynamic to both murine and human EGFR.²⁴ It is engineered by directed evolution through yeast surface display for significantly enhanced affinity for the EGFR. Compared with the wild type EGF, m123 bound 8-fold and 33-fold more tightly to surface EGFR on NR6WT cells and BJ-5a cells, respectively. m123 also bounds 18-fold and 8-fold more tightly to human EGFR and murine EGFR, respectively.²⁴ Interestingly, m123 showed stronger binding at low pH, which is beneficial given that the pH of the TME is universally acidic. Additionally, the binding of m123 to the EGFR may enhance its intracellular degradation, thus benefiting the overall antitumor activity.²⁴

We constructed two versions of this chimeric molecule—the bispecific and trispecific binding engagers. In the bispecific construct, termed BiCEP, OMCP and the m123 are linked via a flexible 20 residue (Gly-Gly-Gly-Gly-Ser)₄ linker and a Myc-tag for ease of detection. In the tri-specific construct, termed TriCEP, a mutated form of

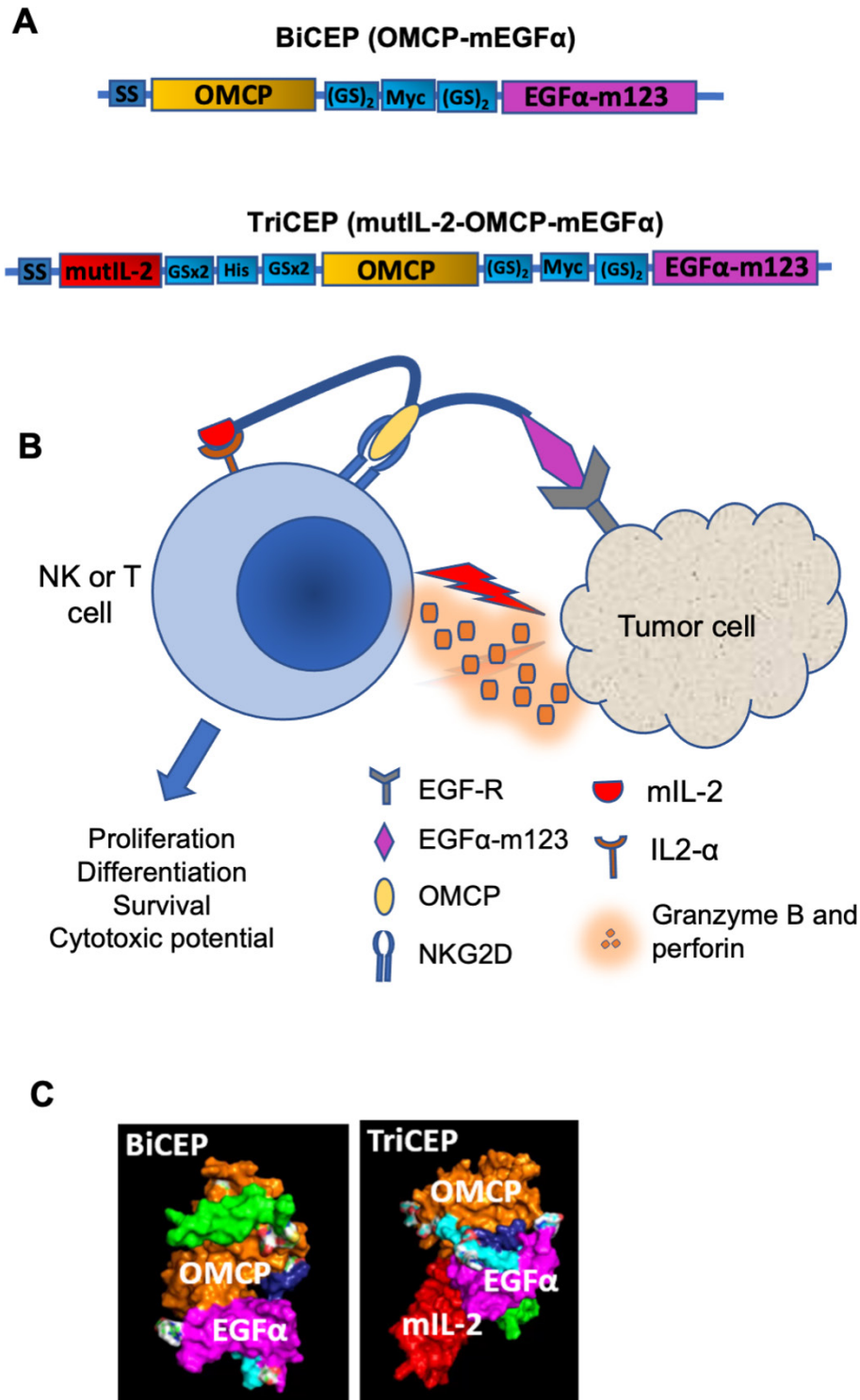


Figure 1 Design of bispecific and trispecific engagers, their anticipated mechanism of action and expression in vitro. (A) Schematic illustration of BiCEP and TriCEP constructs. The composition of the gene cassettes for the chimeric molecules. Each component in the BiCEP (OMCP-EGF α m123) and TriCEP (mutIL-2-OMCP-EGF α m123) is labeled accordingly. SS for signal sequence, (GS)₂ for two copies of GS linker. TriCEP contains the mutant IL-2 (mutIL-2) at the N-terminus. The rest is the same as BiCEP. The actual length of the coding sequence of each component is not proportional to the size of the drawn box. (B) Perceived mechanism of action of the chimeric engagers after being expressed in Tme. The chimeric molecules can engage the NKG2D bearing immune cells, including NK and T cells, with tumor cells through intermolecular binding of EGF α m123 (to EGFR) and OMCP (to NKG2D), and for TriCEP, the flickering action of mutIL-2 on IL-2R to NK or T cell potentiate proliferation and activation. (C) 3D model of protein structures of BiCEP and TriCEP performed using Robetta, indicating no interdomain hindrances. BiCEP, bispecific chimeric engager proteins; EGFR, epidermal growth factor receptor; GS, Gly-Ser; IL-2, interleukin 2; NK, natural killer; OMCP, orthopoxvirus major histocompatibility complex class I-like protein; TriCEP, trispecific chimeric engager protein.

IL-2 (mutIL-2) that has substitutions of alanine for arginine at the 38 position (R38A) and/or lysine for phenylalanine at the 42 position (F42K) is placed upstream of OMCP via a (Gly-Ser-Ser)₄ and a His8-tag for detection. These mutations decrease the affinity of IL-2 for IL-2Ra. This allows mutIL-2 to selectively activate IL-2-signaling only as a tethered form without broadly activating other IL-2R bearing cells and minimizing the unwanted toxicity.²⁵ The hypothesized action mechanisms of BiCEP and TriCEP are illustrated in [figure 1B](#). The simultaneous binding of OMCP to NKG2D and mEGF α to EGFR by the chimeric engagers will efficiently engage the NKG2D bearing NK and T cells with EGFR-bearing tumor cells, bringing the two cells in proximity and creating an immunological synapse. The mutIL-2 in TriCEP would flicker on the IL-2R on the engaged immune cells and enable the activation and proliferation of the engaged NK or T cell to further potentiate the immune response and improve the efficacy.

After the design and construction of BiCEP and TriCEP, we checked for the presence of steric-imposed conformational constraints on both chimeric molecules, and for that, we generated the predicted 3D structure using Robetta protein modeling software.²⁵ The 3D structure in [figure 1C](#) predicts that all the individual components in both chimeric molecules are spatially separated by an intermittent linker, such that they can readily bind to their cognate targets without intradomain steric hindrance. Next, we examined the expression of both BiCEP and TriCEP by transfecting the plasmid constructs to mammalian cells (HEK293 and BHK cells), followed by a Western blot analysis. The results in [figure 2A](#) showed that both chimeric molecules are efficiently expressed and secreted to the supernatant after the molecules are synthesized.

In vitro characterization of BiCEP and TriCEP

Next, we conducted a series of in vitro experiments to test the binding specificity of the individual components in the chimeric molecules to their respective receptors. First, the binding affinity of OMCP to NKG2D was assessed by incubating the TALL-104 cells with the supernatants harvested from HEK293 transfected with the BiCEP and TriCEP constructs for 1 hour at RT. TALL-104 cells are a human leukemic cell line that expresses markers characteristic of both NK cells and cytotoxic T-lymphocytes with high expression of NKG2D.²⁶ The binding of OMCP to NKG2D was determined by measuring the number of cells positive for both NKG2D and the Myc tag contained in both BiCEP and TriCEP (NKG2D⁺/Myc⁺) via flow cytometry analysis. Over 50%–60% of NKG2D⁺ cells are positive for Myc, indicating a good binding affinity of OMCP to NKG2D ([figure 2B](#)).

For determining the binding activity of BiCEP and TriCEP to EGFR, we initially incubated the supernatants with SKOV3 cells for 30 mins at RT. SKOV3 is a human ovarian cancer cell line with overexpression of EGFR.²⁷ The binding of the chimeric molecules to EGFR on the surface of SKOV3 cells was detected by measuring the

number of cells positive for both EGFR and Myc (EGFR⁺/Myc⁺), again via flow cytometry analysis. The result in [figure 2C](#) showed that over 80% of EGFR expressing SKOV3 cells are also positive for Myc, indicating that the mutant form of EGFm123 contained in both BiCEP and TriCEP can efficiently bind to EGFR. No binding was observed with the mock-transfected supernatants, confirming the specificity of this assay. Moreover, from [figure 2C](#), it can be appreciated that approximately 50% of SKOV3 are EGFR negative. These EGFR⁻ SKOV3 cells would serve as an internal control. Importantly, there was no BiCEP or TriCEP binding to these EGFR⁻ cells, indicating the binding specificity of these chimeric molecules to the targeted EGFR.

To further confirm the binding specificity of OMCP and EGFm123 in the two chimeric molecules, we also determined the costaining positivity of EGFR in a murine colon cancer cell line CT26-EGFR that was established in our own lab and has been used in our previous studies in an EGFR-targeted immunotherapy.²⁸ We repeated the binding assay on this cell line with the cell-free supernatants collected from the amplicon infected cells ([figure 2D](#)). From the binding assays, assessed using flow cytometry, there is increased binding of EGF to the truncated human EGFR on the CT26 cell line, evaluated by the cells positive for both Myc and the EGFR. Over 90% of the cells are double positives (EGFR⁺/Myc⁺), indicating that the EGF α binding affinity is retained in the supernatants collected from the amplicon infected cells ([figure 2E](#)). Since the mutIL-2 could only bind weakly to IL-2R, we did not perform any in vitro binding assays on the TriCEP. However, as presented in the following sections, the IL-2 dependent activation by TriCEP could be detected from in vivo studies by the scRNA-seq analysis.

In vitro assay on the ability of BiCEP and TriCEP to engage NK cell with tumor cells and to induce cytotoxicity

To test whether BiCEP and TriCEP could engage NK cells (TALL-104) to kill tumor cells, a real-time in vitro tumor-killing assay was performed.²⁹ Target tumor cells (SKOV3) were incubated with the effector TALL-104 cells at an increasing effector-to-target (E:T) ratio (1:1, 2:1, and 5:1) in the presence or absence of BiCEP or TriCEP. The tumor cell viability was monitored by IncuCyte, a real-time cell imaging device. Images were taken every 2 hours and the number of viable cells per well was quantified with the IncuCyte-FLR-Platform technology ([figure 3A](#)). The cytotoxicity is reported by the percentage of viable cells/percentage of confluence remaining at the end of 24 hours coculture (online supplemental file 1-Fig. S1A). The results show that at the lower E:T ratios (1:1 and 2:1), there is a significant increase in the percentage killing in the presence of BiCEP and TriCEP compared with the control well with the mock-transfected supernatants. However, at the high E:T ratio (5:1), this difference became insignificant. This is probably due to the high background killing activity of TALL-104 cells.³⁰

Fig. 2

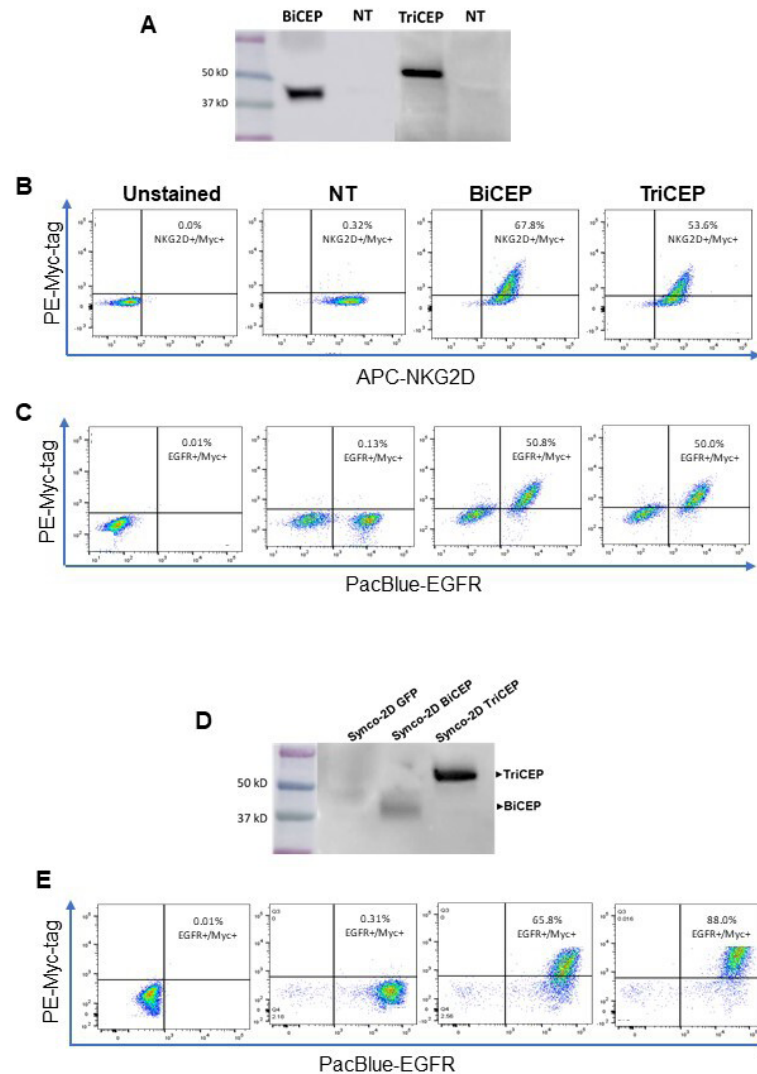
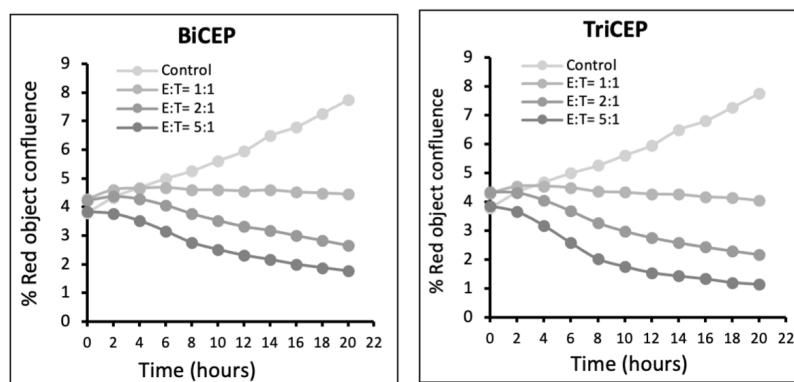


Figure 2 Binding specificity of BiCEP and TriCEP to NKG2D and EGFR. (A) Western blot detection of transgene expression. HEK cells were transfected with pcDNA3.1 plasmids containing GFP, BiCEP and TriCEP constructs or mock-transfected. Supernatant and cell lysate were prepared 48 hours later for Western blot analysis with anti-MYC tag IgG. Lanes 1 and 5, mock-transfected; lanes 2 and 6, GFP; lanes 3 and 7, BiCEP, and lanes 4 and 8, TriCEP. (B) Flow cytometry analysis of the selective binding activity of OMCP to NKG2D on TALL-104 cells. TALL-104 cells were incubated with supernatants harvested from HEK293 cells transfected with mock (NT), BiCEP or TriCEP constructs for one H at room temperature. The cells were then stained with antibodies against NKG2D and Myc-tag and subjected to flow cytometry analysis. The double-positive NKG2D+/Myc+ cells indicate the specific binding of OMCP in the chimeric molecules to NKG2D on TALL-104 cell surface. (C) Binding of EGF α m123 to EGFR on SKOV3 cells. SKOV3 cells were incubated with the same supernatants as in a. the cells were then stained with antibodies against EGFR and Myc-tag and subjected to flow cytometry analysis. The double-positive EGFR+/Myc+ cells indicate the specific binding of EGF α m123 within the chimeric molecules to EGFR on the SKOV3 cell surface. (D) Western-blot analysis to detect the transgene expression. The supernatants collected 48 hours after infection were used for Western blot analysis using anti-MYC IgG and are subsequently used in the assay in the below panel. (E) binding of EGF α m123 to EGFR on CT26-EGFR cells. CT26-EGFR cells were incubated with supernatants harvested from BHK cells infected with mock, Synco-2D BiCEP or Synco-2D TriCEP, for one H at room temperature. The cells were then stained with antibodies against EGFR and Myc-tag and subjected to flow cytometry analysis. The double-positive EGFR+/Myc+ cells indicate the specific binding of EGF α m123 within the chimeric molecules to EGFR on the CT26-EGFR cell surface. BiCEP, bispecific chimeric engager proteins; EGFR, epidermal growth factor receptor; NT, non-transfected; OMCP, orthopoxvirus major histocompatibility complex class I-like protein; TriCEP, trispecific chimeric engager protein.

Moreover, we conducted a highly sensitive FACS (Fluorescence-activated cell sorting) based cleaved caspase 3 cytotoxicity assay using the cleavage of

caspase-3 as a readout of cytotoxicity.²⁸ Briefly, the assay involved labeling of tumor cells (CT26-EGFR cells) with a cell tracker dye, which were then used to coculture

A



B

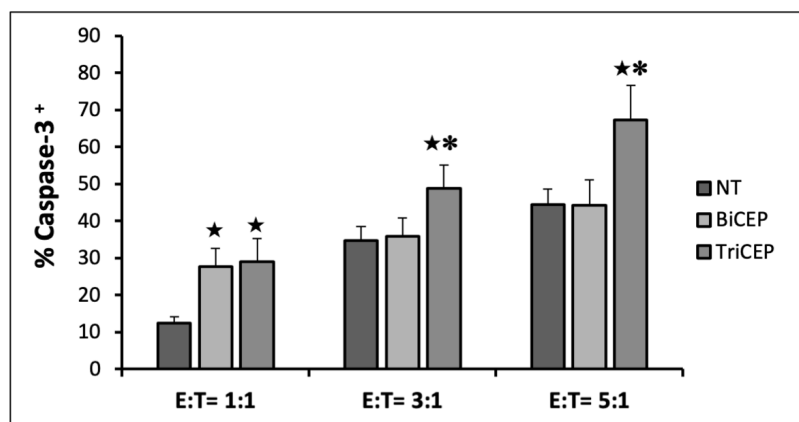


Figure 3 In vitro cytotoxic activity of TALL-104 cells against EGFR-expressing SKOV3 cells in the presence of chimeric engagers. (A) TALL-104 were mixed with SKOV3 tumor cells at the effector-to-target (E:T) ratio of 1:1, 2:1, or 5:1 in triplicates, in a 96 well plate, and in the presence or absence of supernatant harvested from a control vector (NT), or BiCEP and TriCEP. The plate was incubated in the IncuCyte real-time imaging system to monitor cell viability constantly for 48–72 hours. The graphs show the real-time drop in the red object confluence (SKOV3 cells expressing RFP in the nuclei) over 20 hours with BiCEP and TriCEP. One single red object is equivalent to a single viable tumor cell. (B) Quantification of tumor cell killing by FACS based cleaved caspase-3 cytotoxicity assay. The percentage of cleaved caspase-3 as a measure of cytotoxicity is represented by measuring the percentage of caspase-3 positive tumor cells at the end of 4 hour coculture with human primary NK cells. The results are an average of a total of six replicates from two independent assays. ★ $P < 0.05$ as compared with NT control, * $p < 0.05$ as compared with both nt and BiCEP. BiCEP, bispecific chimeric engager proteins; NT, non-transfected; TriCEP, trispecific chimeric engager protein.

with primary human NK cells at different E:T ratios (1:1, 3:1 and 5:1). The cells were permeabilized and stained with an antibody recognizing cleaved caspase 3 and analyzed by flow cytometry (figure 3B, with the detailed data in (online supplemental file 1-Fig.S1B)). The results show that at the lowest E:T ratio (1:1), there is a significant increase on the tumor cell killing (represented as percentage caspase 3 positive cells) in the presence of BiCEP compared with the control well (NT). However, at the high E:T ratios (3:1 and 5:1), this difference became insignificant, probably due to the significant background killing in the control well. There was a significant increase in the tumor cell killing in the presence of TriCEP over the control at all the E:T ratios. Moreover, TriCEP resulted in a better killing than BiCEP at high ratios (3:1 and 5:1).

Insertion of BiCEP and TriCEP coding sequences into an amplicon vector for in vivo delivery

An obvious and common approach to codelivering the chimeric molecules during virotherapy is to insert their coding sequences into the backbone of the OV. However, as HSV has a large genome (over 150 kb) and recombination insertion of foreign genes is cumbersome and time-consuming, thus we chose to use an HSV amplicon vector to deliver these two transgenes. An HSV amplicon is a plasmid-like vector that contains a copy of HSV replication origin (ori-) and packaging signal (pac). In the presence of a helper HSV (eg, an oncolytic HSV), the plasmid gets amplified by a rolling-circle mechanism and the amplified DNA (a total of 150 kb) will be subsequently packaged into a viral particle. Depending on the size of the amplicon plasmid, many copies of the amplicon

sequence (and hence multiple copies of the transgene) can be packaged into each viral particle. So it is an efficient and nimble gene delivery system that we have successfully used in several of our previous studies.³¹ We inserted the coding sequence of either BiCEP or TriCEP, together with a copy of the EGFP (Enhanced Green Fluorescent Protein) gene into the amplicon construct. The inclusion of the EGFP gene allows for easy and convenient titration of the amplicon vector.

We examined the un-packaged amplicon (via transfection of the amplicon plasmid into HEK293 cells) and the packaged amplicon (via infection to BHK cells) for transgene expression (both GFP and the chimeric molecules). For packaging the amplicon plasmids into HSV particles, we initially transfected the amplicon plasmids into BHK cells, which were super-infected 24 hours later with Synco-2D, which is an HSV-1-based OV that has a clear fusogenic property.³² It was constructed by deletion of the ICP34.5. Additionally, it contains two membrane fusion mechanisms—the syn phenotype through mutagenesis and insertion of the truncated form of the gibbon ape leukemia virus envelope fusogenic membrane glycoprotein into the virus genome.³² The generated stock thus contains the mixture of the OV (Synco-2D) and the packaged amplicon. The titer of Synco-2D was determined by the conventional plaque assay and the titer of the packaged amplicon was determined by GFP positive cell counts. The results in [figure 4A](#) showed efficient GFP expression from the amplicon plasmids when they were transfected into BHK cells as they all contain the *EGFP* gene. The extensive appearance of GFP⁺ cells after infection in the bottom panel of [figure 4B](#) indicated that the amplicon plasmid had been efficiently packaged into viral particles when Synco-2D was used as a helper virus (as well as the OV for the in vivo studies) in this unique delivery system, and the estimated amplicon titer from the GFP⁺ cell counting is 1×10^5 per milliliter. The Western blot analysis in [figure 2D](#) showed that the BiCEP and TriCEP molecules were sufficiently produced from the infection of the packaged amplicons.

Therapeutic impact of BiCEP and TriCEP codelivered by amplicon during Synco-2D virotherapy

We chose the CT26-EGFR tumor model for the in vivo studies to evaluate the therapeutic impact of these two chimeric engagers during Synco-2D virotherapy. The experiment process is summarized in [figure 5A](#). Initially, CT26-EGFR tumors were subcutaneously established as reported.²⁸ Once tumors reached the approximate size of 5–6 mm in diameter, they were treated with intratumoral injection of PBS (Phosphate buffered saline), Synco2D-BiCEP, Synco2D-TriCEP, or the control amplicon expressing GFP alone (Synco-2D-GFP) at 5×10^6 pfu of Synco-2D per mice. Tumors were measured every other day using calipers and tumor volumes were calculated as described in the Materials and Methods. The results showed that, while Synco-2D-GFP only showed a marginally therapeutic effect against this murine tumor, both

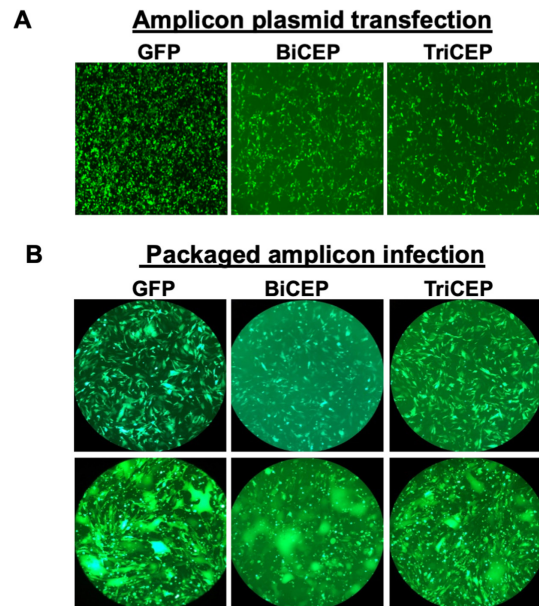


Figure 4 Characterization of amplicon plasmids the chimeric engagers and production of the packaged amplicon. (A) Transfection efficiency as determined by EGFP expression in BHK cells transfected with amplicon plasmid constructs: Amplicon-GFP, Amplicon-BiCEP, or Amplicon-TriCEP (all contain the *EGFP* gene). (B) Amplicon packaging efficiency as determined by EGFP expression in cells infected with the same packaged amplicons. For amplicon packaging, the same amplicon plasmids were transfected into BHK cells. Micrographs were taken at 24 hours (the top panel) before the cells were super-infected with Synco-2D (one pfu/cell). The packaged amplicons were harvested 24 hours later and used to infect fresh BHK cells, and the packaging efficiency was determined by the GFP expression after infection (the bottom panel). BiCEP, bispecific chimeric engager proteins; TriCEP, trispecific chimeric engager protein.

Synco2D-BiCEP and Synco2D-TriCEP produced a significantly better therapeutic effect compared with the PBS control ([figure 5B](#)). By the end of the experiment, all mice were euthanized, and the tumor explanted ([figure 5C](#)). The measurement of explanted tumors confirmed the enhanced therapeutic efficacy by the codelivery of both the BiCEP and TriCEP molecules. The transgene expression by the codelivered amplicons during virotherapy was confirmed by examining the GFP expression in tumor sections collected 2 days after virotherapy ([figure 5D](#)).

Characterization of immune cell landscape in TME during virotherapy with or without codelivery of TriCEP by scRNA-seq

The previous studies on characterizing the infiltrating immune cells during virotherapy are fragmented, as they were designed to focus on certain populations of immune cells.^{12 13 33} Hence, we decided to use scRNA-seq to fully characterize the immune cell landscape as well as their activation status during Synco-2D virotherapy with or without the amplicon-mediated codelivery of TriCEP. We decided not to include BiCEP in this scRNA-seq analysis as it was similarly constructed as TriCEP. The scheme for this scRNA-seq is shown in [figure 6A](#). BALB/c mice bearing

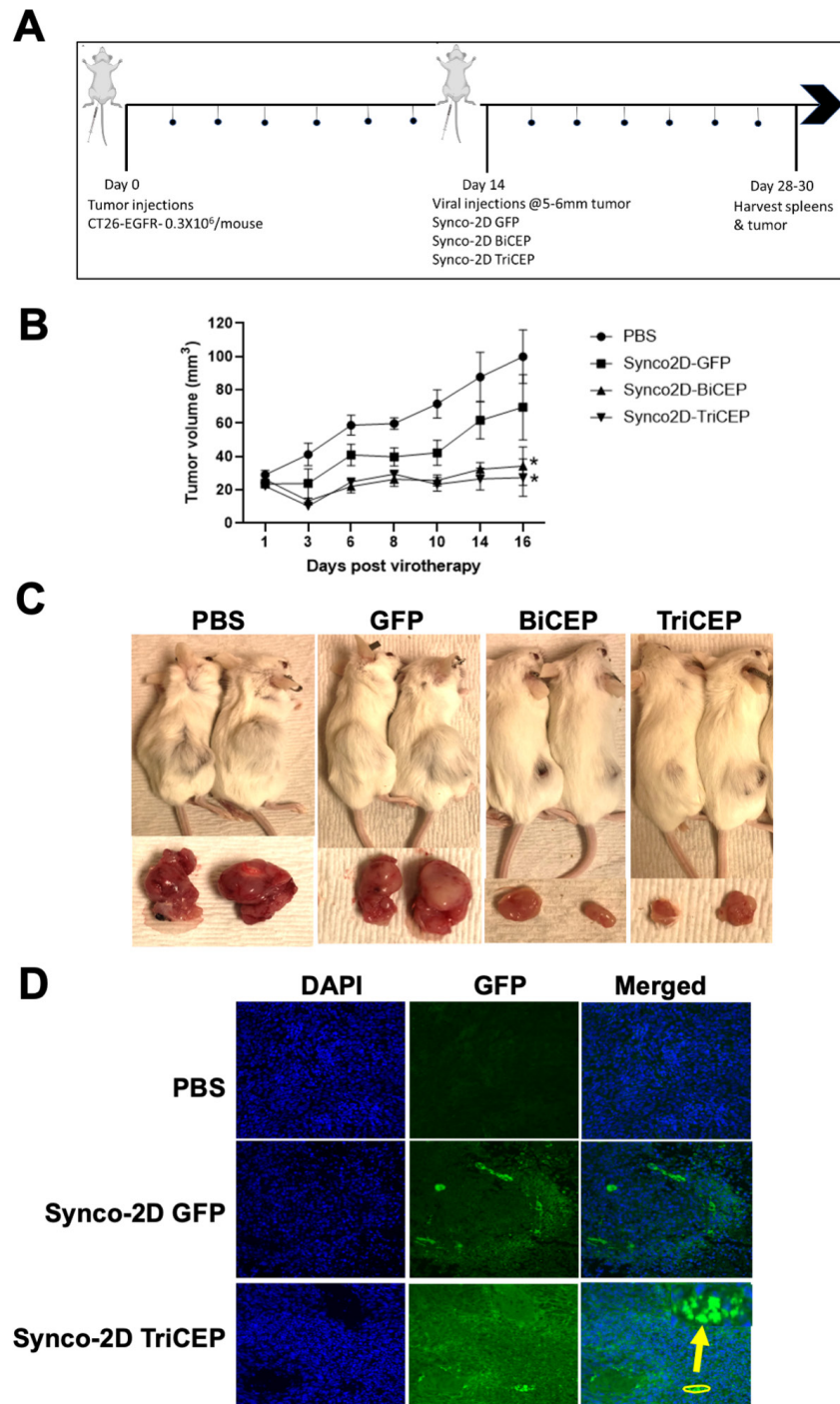


Figure 5 Therapeutic evaluation of coadministration of the chimeric engagers with Synco-2D in a murine colon cancer model. (A) Treatment scheme of BALB/c mice bearing CT26-EGFR subcutaneous tumors. 3×10^5 CT26-EGFR cells were injected into the right flank of 6–8 week old female BALB/c mice. When the tumors reached the approximate size of 6–8 mm, mice were randomly grouped and treated with 5×10^6 pfu Synco-2D, Synco-2D GFP, Synco-2D BiCEP, or Synco-2D TriCEP. PBS group served as a negative control. (B) Tumor growth curve after virotherapy. * $P < 0.05$ as compared with the PBS control and Synco-2D GFP treatment. (C) Representatives of the tumor-bearing mice and the gross appearance of tumors excised at the end of the experiment. (D) Representative immunohistochemical and histologic images from tumor sections were obtained 48 hours after mice receiving the different treatment. GFP is indicative of expression of the transgene and was detected in the tumor samples from Synco-2D GFP and Synco-2D TriCEP treatment (exemplified in an enlarged inset). BiCEP, bispecific chimeric engager proteins; EGFR, epidermal growth factor receptor; TriCEP, trispecific chimeric engager protein.

subcutaneous CT26-EGFR tumors (approx. 8–10 mm in diameter) were injected intratumorally with either PBS, Synco2D-TriCEP, or Synco-2D-GFP at 5×10^6 pfu per mice

(figure 6A). Forty-eight hours later, the tumors were excised from the mice and dissociated into a single-cell suspension. Due to the rarity of immune cell filtration in

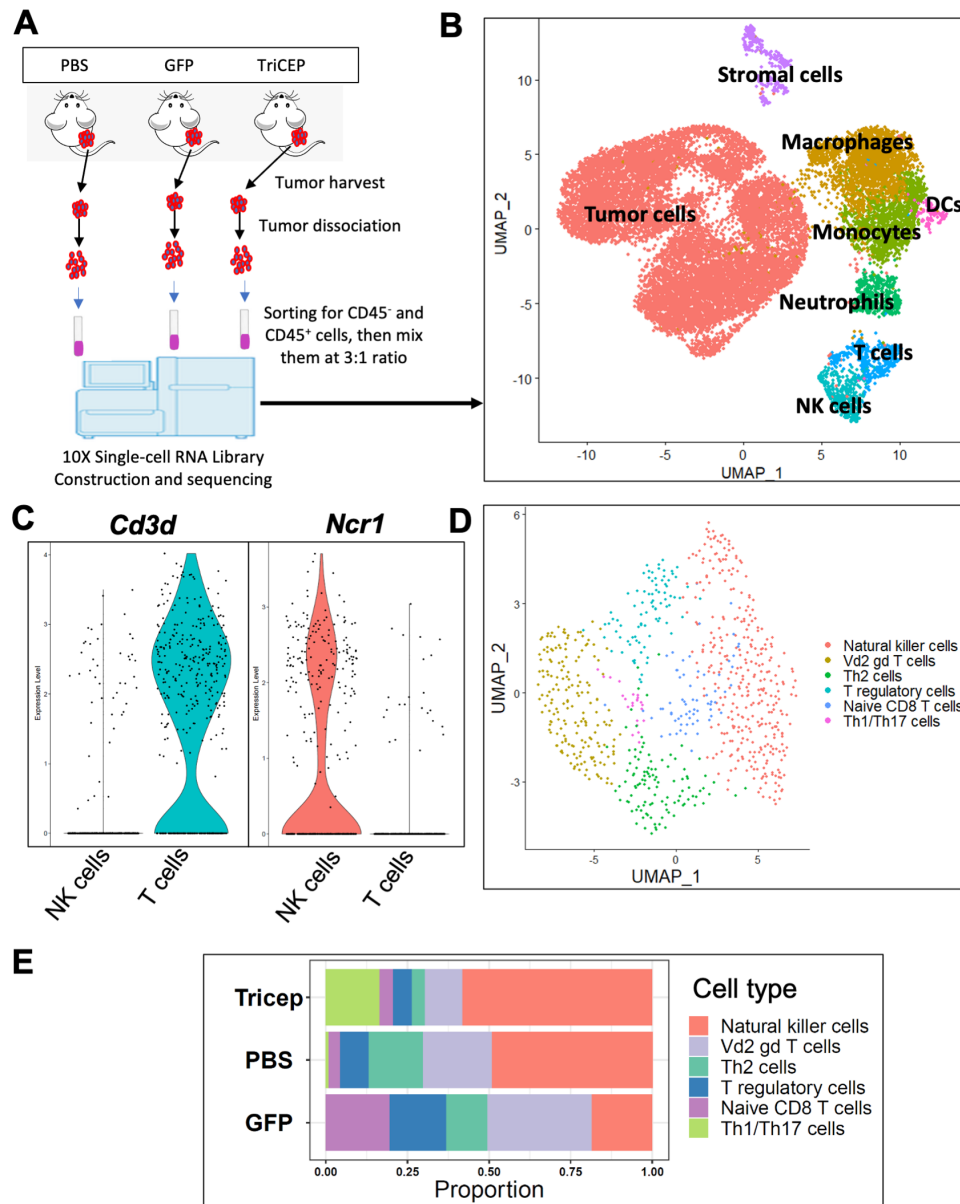


Figure 6 scRNA-seq characterization of infiltrating immune cells in TME after different treatment. (A) Experimental setup of scRNA-seq on tumor samples. Tumors were explanted from three mice from each group 48 hours after receiving the indicated treatment and pooled into a single tube for each treatment Group. The pool tumors were then digested using a tissue dissociation kit and gentleMACS tissue dissociator from Miltenyi. The dissociated cells were sorted into CD45⁻ and CD45⁺ populations and were then mixed at a 3:1 ratio to proceed to scRNA-seq using a 10X genomics pipeline. (B) UMAP presentation of major cell types classified into tumor cells and six distinct clusters of immune cells are indicated. (C) Violin plots of representative cluster-specific marker genes (*Cd3d* and *Ncr1* for T and NK cells, respectively). (D) Subclustering of T and NK cells annotated by mapping the scRNA seq data to Monaco immune database. (E) The relative composition and proportion of T and NK cell subclusters within each treatment group (PBS, Synco-2D- GFP (GFP), Synco-2D-TriCEP (TriCEP)). DC, dendritic cell; NK, natural killer; scRNA-seq, single-cell RNA sequence; TME, tumor microenvironment; UMAP, uniform manifold approximation and projection.

the TME, we initially sorted the single cells into CD45⁻ and CD45⁺ populations, which were subsequently mixed at a 3:1 ratio for single cell capture, barcoding, and sequencing by the 10× Genomics Chromium pipeline.

For characterizing the types of infiltrating immune cells in the TME of the collected tumor samples after treatment, all cells were initially clustered into unbiased cell-type classification using the Seurat package,^{34–36} as shown in figure 6A. Tumor cells were clustered by CD45⁻ and

hEGFR⁺ expression. CD45⁺ cells were clustered based on the assessment of known cell type markers into distinct lymphoid; monocyte/macrophage, T cells, NK cells, DCs, and neutrophils (figure 6B). For the purpose of this study, we restricted our analysis to NK and T cells, which are the main effector cells targeted by these chimeric engagers. Cell-type specific gene expression of *Cd3d* for T cells and *Ncr1* for NK cells are shown in the violin plots (figure 6C). The T and NK cells are further subclustered

into six distinct clusters (NK cells, Vd2 gd T cells, Th2 cells, T regulatory cells, Naïve CD8⁺ T cells and Th1/Th17 cells) (figure 6D).³⁷ The subclustering was then stratified by samples to illustrate the relative composition of each subtype of these infiltrating NK and T cells in the different groups (figure 6E). The data showed that Synco-2D-TriCEP treatment increased the proportion of NK cells in TME. Considering that the proportion of CD45⁺ cells in tumors treated with Synco-2D-TriCEP was significantly higher than in the other two groups (data not shown), the increase in NK cells is quite significant. Moreover, treatment with Synco-2D-TriCEP generated more favorable T cell responses. First, it increased the proportion of Th1/Th17 cells by approximately twofold and fourfold compared with PBS and GFP, respectively. Second, it reduced the relative presence of both Th2 (approx. twofold and fourfold reduction compared with PBS and GFP, respectively) and Treg cells (approx. twofold reduction compared with both control groups). Both of these changes on T cells in TME are considered desirable for cancer immunotherapy.

To determine the activation status of the infiltrating NK and T cells in the TME, we analyzed the expression of the activation and major cytotoxic effector markers of NK and T cells, including *Klrk1* (NKG2D), *Cd69* (Cluster of Differentiation 69), *Stat3* (Signal transducer and activator of transcription 3) *Prf1* (perforin), and *Gzmb* (granzyme B) (figure 7A–E). Among them, *Cd69* is an activation marker for both T and NK cells.³⁸ Although NKG2D is constitutively expressed on both NK and CD8⁺ T cells, its expression is enhanced when these cells become activated.³⁹ As such, it is also considered as an activation marker for both cell types. *Stat3* is a transcription factor that is activated downstream of many key cytokine receptors expressed by lymphocytes. As such, the presence of *Stat3* is indicative of the activated status of immune cells. Moreover, it plays an important role in regulating NK cell function and is thus considered as a NK cell activation marker (figure 7C). Perforin and granzyme B are classical markers for critical cytolytic enzymes for both NK and T cells and their expression levels indicate their cytolytic activity.⁴⁰ The expression of all these genes was significantly elevated in the tumors treated by Synco-2D TriCEP as compared with the other two groups with the $p < 0.05$ (figure 7D,E), indicating that TriCEP directly contributed to the activation and/or effector function of NK and T cells.

In addition to the above activation markers, we also analyzed the expression of key cytokines in the infiltrated NK and T cells shown in (online supplemental file 1-Fig.S2), including *Icos* (online supplemental file 1-Fig.S2A), *Ifng* (online supplemental file 1-Fig.S2B) and *Tgfb1* (online supplemental file 1-Fig.S2C). The expression of these cytokines is significantly elevated in NK cells, whereas significant expression of *Icos* and *Tgfb1* is only observed within the T cell clusters in the TriCEP treated group (compared to the PBS control. The p values for the violin plots showing activation genes and

cytokine genes are shown in (online supplemental file 1-Fig. S2D).

DISCUSSION

It is becoming increasingly clear that combining virotherapy with immunotherapy can bring a synergistic therapeutic effect against solid tumors. One approach is to take advantage of the induced change in the landscape of the infiltrating immune cells during virotherapy by codelivering bispecific engagers that can direct T cells or NK cells to attack tumor cells. Here, we report the design of a class of novel chimeric engagers—BiCEP and TriCEP. Unlike the approaches reported in previous studies that engage either T cells or NK cells separately, BiCEP and TriCEP can simultaneously engage both types of these two important immune cells for cancer immunotherapy. Additionally, we chose to engage NKG2D on the immune cells instead of CD3 that is the predominant target for most of the BiTEs reported in the literature. In addition to the abundant expression on NK cells, NKG2D is expressed on CD8⁺ and $\gamma\delta$ T cells in humans.¹⁹ In contrast, CD3 is expressed on all T cell subsets, including regulatory T cells. As such, BiCEP and TriCEP may have the additional advantage of selectively engaging CD8⁺ T cells and $\gamma\delta$ T cells, potentiating their antitumor effect through co-stimulation to enhance T-cell receptor activation.²⁶ Our in vitro data, on both human tumor cells that naturally express EGFR or murine tumor cells that were transduced with the human *EGFR* gene, showed that both BiCEP and TriCEP could guide cells with NK and T cell property to kill these tumor cells that express the targeted tumor antigen. Codelivery of BiCEP and TriCEP in vivo through an amplicon vector has significantly enhanced the therapeutic effect of an HSV-1-based OV, Synco-2D, against a murine colon cancer that is otherwise only moderately permissive to the oncolytic effect of the virus. Efforts are currently underway to insert one of these engaging molecules (TriCEP) into the oncolytic viral genome, which will allow for more efficient transgene expression and hence for a better in vivo therapeutic effect. As part of the path for clinical translation of this armed strategy, the new virus will be tested in more than one tumor model that will include those expressing native EGFR.

BiTEs are commonly constructed by linking two scFvs, with one binding to a key receptor on the immune cells and the other to a TAA on tumor cells.^{41 42} We chose to use two ligand-based polypeptides instead. One of them is OMCP, which can selectively bind to NKG2D of both human and rodent origin with an affinity similar to or even higher than its natural ligand.²³ The other one is a mutant form of EGF, m123, which can bind to EGFR of both human and murine origin with an enhanced affinity.²⁴ Our chimeric engager design on using these unique ligands instead of scFvs thus theoretically has two potential advantages. First, both ligands can bind their receptors from either human or murine origin. This

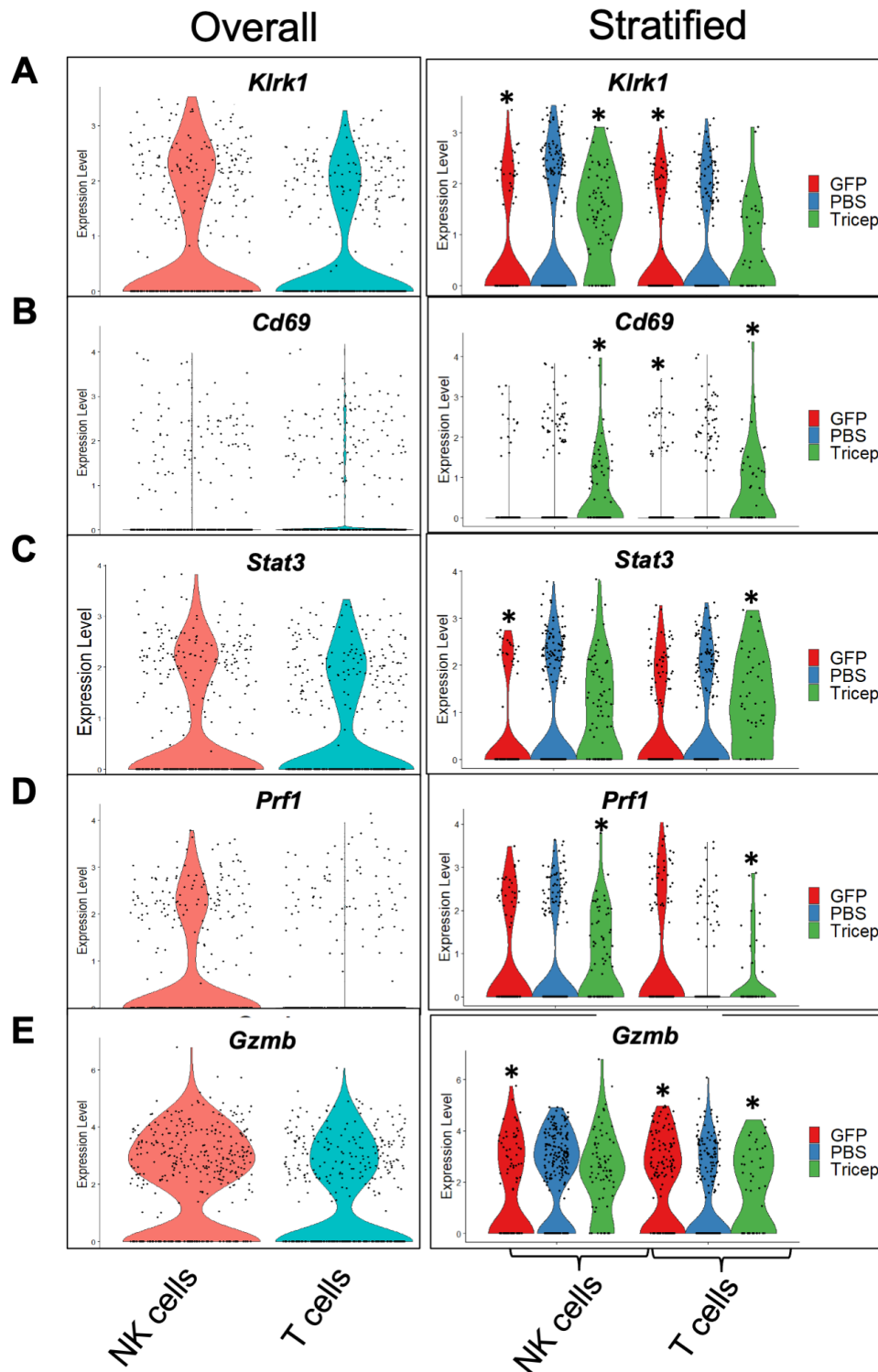


Figure 7 Quantification of the signature NK and T cell activation and cytotoxic genes by scRNA-seq. (A) Violin plots showing the expression of *Klrk1* (A), *Cd69* (B), *Stat3* (C), *Prf1* (D) and *Gzmb* (E) within NK and T cell cluster (overall) and further stratification as per the treatment group (PBS, GFP or TriCEP). * $P < 0.05$ as compared with PBS control. TriCEP, trispecific chimeric engager protein.

allows these chimeric molecules to be tested on immune cells of both human and murine sources, making the outcomes more clinically relevant. Second, as ligands usually have lower binding affinity than scFvs, this may make these engagers less likely to induce cytokine storms during clinical application. Indeed, it has been suggested

that tuning down of the binding affinity may be necessary to increase the safety for both CAR-T cell and BiTE immunotherapy for clinical application.²¹

Several cell surface-expressed TAAs have been chosen as the targets for BiTE-mediated cancer immunotherapy.⁴³ EGFR is overexpressed on many carcinomas and hence

is a good therapeutic target for an immune engager such as the BiCEP and TriCEP. However, EGFR is also widely expressed on many normal tissues,⁴⁴ which poses a risk of potential on-target off-tumor toxicity. Delivery of BiCEP and TriCEP by an HSV amplicon vector as reported in our studies can partly limit such potential toxicity as amplicon relies on the helper virus (in this case, it is the Synco-2D OV) for further replication and packaging *in vivo*. However, for the best control of the expression of these engagers to tumor tissues, we may need to insert their coding sequences into the backbone of the viral genome of the OV, using a strict late viral promoter. Our previous studies have shown that a strict late viral promoter such as the UL38p controls transgene expression strictly to the tumor tissues in the context of an oncolytic HSV.⁴⁵ scRNA-seq, owing to its capability at revealing complex and rare cell populations, uncovering regulatory relationships between genes, and tracking the trajectories of distinct cell lineages in development,⁴⁶ has been widely used in recent years in many studies where these intricate characterizations are desirable.⁴⁷ However, to our knowledge, scRNA-seq has not yet been applied to characterize the infiltration of immune cells and their activation status during virotherapy. We thus conducted an scRNA-seq analysis of tumor samples collected from some of the treatment groups. The data revealed that virotherapy could increase and/or alter the infiltrating immune cells in a way that is consistent with the previous report that OVs can covert cold tumors into hot ones. Co-administration of the chimeric engagers can further enhance this effect. Most importantly, the engagers can contribute to the activation of the infiltrated immune cells, clearly indicating its role in engaging and potentiating these immune cells to attack tumor cells. Comprehensive data on scRNA-seq analysis of immune cell infiltration by comparing several oncolytic virotherapies will soon be submitted separately for publication.

MATERIALS AND METHODS

Cell lines and OV

HEK293, SKOV3, CT26, Vero, BHK, TALL-104 cells were obtained from ATCC. CT26-EGFR cells were established from CT26 cells by stably transducing the cells with a lentiviral vector that contains EGFR extracellular and transmembrane domains without the intracellular sequence.¹⁷ All cells were cultured as described in online supplemental file 2. Synco-2D is an HSV-1-based OV. Its construction has been described in our previous publications.³²

Plasmid construction

For building the BiCEP, the coding sequence for OMCP (1–152) and the mutated form of EGF α (m123), together a glycine/serine linker and a Myc tag was synthesized by GenScript (U0596DB120; U0596DB130) is inserted in the frame for ease of detection. TriCEP coding sequence was similarly synthesized, except that the coding sequence

for a mutated form of IL-2 was added to the 5' end. Both synthesized sequences were cloned into pcDNA3.1 plasmid to generate pcDNA3.1-BiCEP and pcDNA3.1-TriCEP, respectively.

Amplicon plasmid cloning and amplicon production

For constructing amplicon plasmids containing these two chimeric engagers, the key components of an HSV amplicon, the Ori and the Pac signals, together with the EGFP coding sequence, were cut from pW7-EGFP, which is an amplicon that our lab had constructed and used in many of our previous studies.³¹ The cut-out fragment containing the amplicon components was then cloned into pcDNA3.1-BiCEP and pcDNA3.1-TriCEP, to generate Amplicon-BiCEP and Amplicon-TriCEP, respectively. The procedure for packaging amplicons is described in online supplemental file 2. The generated stocks of viruses were labeled as Synco-2D-GFP, Synco-2D-BiCEP, and Synco-2D-TriCEP, respectively, and stored at -80°C until use.

In vitro detection of transgene expression in mammalian cells

For determining the transgene expression from either the amplicon plasmids or from the packaged amplicons, HEK293 cells were transfected with pW7-GFP, Amplicon-BiCEP and Amplicon-TriCEP, and BHK cells were infected with the corresponding packaged amplicons. The supernatants were collected 48 and 72 hours later. The collected supernatants were either used directly or concentrated using 10000 MWCO Millipore spin-columns and stored at -80°C before they were used for Western blot detection or other quantitative assays. Ponceau staining was performed on the gels loaded with supernatant samples to ensure a near equal sample loading.

Binding assays by flow cytometry analysis

The binding of OMCP to NKG2D on immune cells (TALL-104) and EGF α to EGFR on tumor cells (SKOV3) were determined by incubating the cells with the supernatants collected from HEK293 cells transfected with the amplicon plasmids or BHK cells infected with the packaged amplicon as described above. The experimental procedure for conducting the assay is detailed in online supplemental file 2. The binding of OMCP to NKG2D and EGF α to EGFR on the cells is determined by the detection of NKG2D⁺/Myc⁺ and EGF α ⁺/Myc⁺ double-positive cells by flow cytometry, respectively.

In vitro coculture killing assay

Ovarian cancer cells (SKOV3) were cocultured with TALL-104 cells, at a different E:T ratios (1:1, 2:1, and 5:1) for 2–3 days. Tumor cell lysis was monitored in real-time using real-time fluorescent microscopy (IncuCyte; Essen Biosciences). The cytotoxicity is reported by the percentage of viable cells/percentage of confluence remaining at the end of 48-hour coculture.

Caspase 3 assay setup and antibody staining

DDAO-SE (CellTrace Far Red dye- C34564) labeled target cells (CT26-EGFR) were seeded at 100,000 cells per well

in a 96-round bottom tissue culture plate and cocultured with human primary NK cells at E:T ratios of 1:1, 3:1 and 5:1. The cells were incubated O/N at 37°C, 5% CO₂ in a humidified incubator for 3–4 hours. The cells were then washed, trypsinized, fixed and permeabilized with Fix/Perm solution (BD Biosciences) and stained for cleaved caspase 3. The stained cells were then prepared for flow cytometric analysis. The detailed procedure is described in online supplemental file 2.

OV and amplicon titration

Vero cells in 12-well plates were infected with serially diluted stocks in triplicates. The titer of Synco-2D is determined by plaque-forming units counted 24–48 hours later. The amplicon titer is determined by counting the number of GFP⁺ cells. In most stock preparations, the Synco-2D to amplicon ratio is approximately 8–10:1.

Western blot

Whole-cell lysates and supernatants from either transfected or infected cells were analyzed by following standard procedures for western blot. The primary antibody used for the detection of chimeric proteins is Myc-tag (1:2000) (Cell Signaling Technology, Danvers, Massachusetts, USA) and an HRP-labeled secondary antibody (anti-rabbit IgG, HRP linked Antibody) at 1:1000 dilution.

Animal studies

Immune-competent female BALB/c mice (4–6 weeks old) were purchased from Charles River Laboratories. All animal experiments were approved by the University's Institutional Animal Care and Use Committee. 3×10^5 CT26-EGFR cells were injected subcutaneously to the shaved right flank of the mice. Once the tumor volumes reached the approximate size of 6 mm in diameter, eight mice were randomized into different groups to receive either PBS control or Synco-2D treatment with or without the chimeric molecule-containing amplicons, at the dose of 5×10^6 pfu Synco-2D per mouse. Three mice from groups receiving the treatment of PBS, Synco-2D GFP and Synco-2D TriCEP were euthanized on day 3 after virotherapy to collect tumor tissues for scRNA-seq or histology exam and spleens for other immune assays. The rest of the mice (n=5) were kept for 2–3 weeks to monitor tumor growth by measuring two perpendicular tumor diameters with a caliper. Tumor volume was calculated by the formula: tumor volume (mm³) = [length (mm)] × [width (mm)]² × 0.52.

H&E staining and immunohistochemistry

Tumor tissues were fixed and embedded in paraffin and sections were prepared. H&E staining was performed as per standard procedures and as detailed in online supplemental file 2. The primary antibody used to stain the sections is GFP (Santa Cruz Biotech, Dallas, Texas, USA).

Tumor dissociation and single-cell processing

For scRNA-seq studies, the freshly collected tumors were immediately immersed in a tissue storage medium

(Miltenyi, San Diego, California, USA) and kept at 4°C until ready for dissociation. Within 24 hours, tissues were processed to single-cell suspensions using the human tumor dissociation kit from Miltenyi and the gentleMACS apparatus and this was done by following the manufacturer's protocol. Single-cell suspensions were then stained with a fluorescently conjugated antibody specific to CD45 (BioLegend) for 30 min at 4°C. The cells were washed with cell staining buffer (BioLegend) and CD45⁺ live cells were sorted on a FACS Melody cell sorter (BD) into 2%FBS in PBS, which were kept on ice until the cells were further processed for scRNA-seq (scRNA-seq library preparation and sequencing, transcriptome analysis and single-cell data analysis)^{48–50} are included as online supplemental file 2.

Statistical analysis

All quantitative results are displayed as the mean±SD.D. The statistical difference between the two groups was compared using a Mann-Whitney U test or a Student's t-test. If more than two groups were compared, analysis of variance was used. Statistical analysis was determined using Prism V.5 software (GraphPad Software, La Jolla, California, USA). A p <0.05 was considered statistically significant.

Contributors DR and XZ conceived, designed the experiments. DR executed all the experiments in the study. BM ran the sequencing and preprocessed the data for analysis. GP and DR performed bioinformatics analysis. DR and XZ wrote the manuscript.

Funding This work was supported by the CPRIT grant RP200464 and a grant from the William and Ella Owens Medical Research Foundation (to XZ). We thank Dr. Xinli Liu for assistance with the cell sorting and Drs. Weiyi Peng and Navin Varadarajan for advice.

Competing interests None declared.

Patient consent for publication Not required.

Provenance and peer review Not commissioned; externally peer reviewed.

Data availability statement Data are available on reasonable request. The data that support the findings of this study are either contained in online supplemental files or available from the authors on request.

Supplemental material This content has been supplied by the author(s). It has not been vetted by BMJ Publishing Group Limited (BMJ) and may not have been peer-reviewed. Any opinions or recommendations discussed are solely those of the author(s) and are not endorsed by BMJ. BMJ disclaims all liability and responsibility arising from any reliance placed on the content. Where the content includes any translated material, BMJ does not warrant the accuracy and reliability of the translations (including but not limited to local regulations, clinical guidelines, terminology, drug names and drug dosages), and is not responsible for any error and/or omissions arising from translation and adaptation or otherwise.

Open access This is an open access article distributed in accordance with the Creative Commons Attribution Non Commercial (CC BY-NC 4.0) license, which permits others to distribute, remix, adapt, build upon this work non-commercially, and license their derivative works on different terms, provided the original work is properly cited, appropriate credit is given, any changes made indicated, and the use is non-commercial. See <http://creativecommons.org/licenses/by-nc/4.0/>.

ORCID iDs

Guangsheng Pei <http://orcid.org/0000-0003-1804-7598>

Zhongming Zhao <http://orcid.org/0000-0002-3477-0914>

Xiaoliu Zhang <http://orcid.org/0000-0002-2085-3997>

REFERENCES

- 1 Koch MS, Lawler SE, Chiocca EA. Hsv-1 oncolytic viruses from bench to bedside: an overview of current clinical trials. *Cancers* 2020;12:3514.
- 2 Bishnoi S, Tiwari R, Gupta S, et al. Oncotargeting by vesicular stomatitis virus (VSV): advances in cancer therapy. *Viruses* 2018;10:90.
- 3 Peter M, Kühnel F. Oncolytic adenovirus in cancer immunotherapy. *Cancers* 2020;12:3354.
- 4 Torres-Domínguez LE, McFadden G. Poxvirus oncolytic virotherapy. *Expert Opin Biol Ther* 2019;19:561–73.
- 5 Msaouel P, Opyrchal M, Dispenzieri A, et al. Clinical trials with oncolytic measles virus: current status and future prospects. *Curr Cancer Drug Targets* 2018;18:177–87.
- 6 Conry RM, Westbrook B, McKee S, et al. Talimogene laherparepvec: first in class oncolytic virotherapy. *Hum Vaccin Immunother* 2018;14:839–46.
- 7 Bommareddy PK, Shettigar M, Kaufman HL. Integrating oncolytic viruses in combination cancer immunotherapy. *Nat Rev Immunol* 2018;18:498–513.
- 8 Sun L, Funchain P, Song JM, et al. Talimogene Laherparepvec combined with anti-PD-1 based immunotherapy for unresectable stage III–IV melanoma: a case series. *J Immunother Cancer* 2018;6:36.
- 9 Ma J, Ramachandran M, Jin C, et al. Characterization of virus-mediated immunogenic cancer cell death and the consequences for oncolytic virus-based immunotherapy of cancer. *Cell Death Dis* 2020;11:48.
- 10 Bartlett DL, Liu Z, Sathiah M, et al. Oncolytic viruses as therapeutic cancer vaccines. *Mol Cancer* 2013;12:103.
- 11 Hamid O, Hoffner B, Gasal E, et al. Oncolytic immunotherapy: unlocking the potential of viruses to help target cancer. *Cancer Immunology, Immunotherapy* 2017;66:1249–64.
- 12 Fu X, Rivera A, Tao L, et al. An HSV-2 based oncolytic virus can function as an attractant to guide migration of adoptively transferred T cells to tumor sites. *Oncotarget* 2015;6:902–14.
- 13 Ribas A, Dummer R, Puzanov I, et al. Oncolytic virotherapy promotes intratumoral T cell infiltration and improves anti-PD-1 immunotherapy. *Cell* 2017;170:e10:1109–19.
- 14 Yu F, Wang X, Guo ZS, et al. T-Cell engager-armed oncolytic vaccinia virus significantly enhances antitumor therapy. *Mol Ther* 2014;22:102–11.
- 15 Freedman JD, Hagel J, Scott EM, et al. Oncolytic adenovirus expressing bispecific antibody targets T-cell cytotoxicity in cancer biopsies. *EMBO Mol Med* 2017;9:1067–87.
- 16 Speck T, Heidbuechel JPW, Veinalde R, et al. Targeted bite expression by an oncolytic vector augments therapeutic efficacy against solid tumors. *Clin Cancer Res* 2018;24:2128–37.
- 17 Fu X, Tao L, Wu W, et al. Arming HSV-Based Oncolytic Viruses with the Ability to Redirect the Host's Innate Antiviral Immunity to Attack Tumor Cells. *Mol Ther Oncolytics* 2020;19:33–46.
- 18 Raulet DH. Roles of the NKG2D immunoreceptor and its ligands. *Nat Rev Immunol* 2003;3:781–90.
- 19 Prajapati K, Perez C, Rojas LBP, et al. Functions of NKG2D in CD8⁺ T cells: an opportunity for immunotherapy. *Cell Mol Immunol* 2018;15:470–9.
- 20 Sigismund S, Avanzato D, Lanzetti L. Emerging functions of the EGFR in cancer. *Mol Oncol* 2018;12:3–20.
- 21 Yu S, Yi M, Qin S, et al. Next generation chimeric antigen receptor T cells: safety strategies to overcome toxicity. *Mol Cancer* 2019;18:125.
- 22 Kamperschroer C, Shenton J, Lebrec H, et al. Summary of a workshop on preclinical and translational safety assessment of CD3 bispecifics. *J Immunotoxicol* 2020;17:67–85.
- 23 Campbell JA, Trossman DS, Yokoyama WM, et al. Zoonotic orthopoxviruses encode a high-affinity antagonist of NKG2D. *Journal of Experimental Medicine* 2007;204:1311–7.
- 24 Lahti JL, Lui BH, Beck SE, et al. Engineered epidermal growth factor mutants with faster binding on-rates correlate with enhanced receptor activation. *FEBS Lett* 2011;585:1135–9.
- 25 Ghasemi R, Lazear E, Wang X, et al. Selective targeting of IL-2 to NKG2D bearing cells for improved immunotherapy. *Nat Commun* 2016;7:12878.
- 26 Bauer Set al. Activation of NK cells and T cells by NKG2D, a receptor for stress-inducible MICA. *Science* 1999;285:727–9.
- 27 Wang K, Li D, Sun L. High levels of EGFR expression in tumor stroma are associated with aggressive clinical features in epithelial ovarian cancer. *Onco Targets Ther* 2016;9:377–86.
- 28 He L, Hakimi J, Salha D, et al. A sensitive flow cytometry-based cytotoxic T-lymphocyte assay through detection of cleaved caspase 3 in target cells. *J Immunol Methods* 2005;304:43–59.
- 29 Lanigan TM, Rasmussen SM, Weber DP, et al. Real time visualization of cancer cell death, survival and proliferation using fluorochrome-transfected cells in an IncuCyte® imaging system. *J Biol Methods* 2020;7:e133.
- 30 Kruse CA, Visonneau S, Kleinschmidt-DeMasters BK, et al. The human leukemic T-cell line, TALL-104, is cytotoxic to human malignant brain tumors and traffics through brain tissue: implications for local adoptive immunotherapy. *Cancer Res* 2000;60:5731–9.
- 31 Zhang X, Alwis MD, Hart SL, et al. High-Titer recombinant adeno-associated virus production from replicating amplicons and herpes vectors deleted for glycoprotein H. *Hum Gene Ther* 1999;10:2527–37.
- 32 Nakamori M, Fu X, Pettaway CA, et al. Potent antitumor activity after systemic delivery of a doubly fusogenic oncolytic herpes simplex virus against metastatic prostate cancer. *Prostate* 2004;60:53–60.
- 33 Chon HJ, Lee WS, Yang H, et al. Tumor microenvironment remodeling by intratumoral oncolytic vaccinia virus enhances the efficacy of Immune-Checkpoint blockade. *Clin Cancer Res* 2019;25:1612–23.
- 34 Vieth B, Parekh S, Ziegenhain C, et al. A systematic evaluation of single cell RNA-seq analysis pipelines. *Nat Commun* 2019;10:4667.
- 35 Stuart T, Butler A, Hoffman P, et al. Comprehensive integration of single-cell data. *Cell* 2019;177:e21:1888–902.
- 36 McInnes L, Healy J, Saul N, et al. UMAP: uniform manifold approximation and projection. *Journal of Open Source Software* 2018;3:861.
- 37 Aran D, Looney AP, Liu L, et al. Reference-Based analysis of lung single-cell sequencing reveals a transitional profibrotic macrophage. *Nat Immunol* 2019;20:163–72.
- 38 Cibrián D, Sánchez-Madrid F. Cd69: from activation marker to metabolic gatekeeper. *Eur J Immunol* 2017;47:946–53.
- 39 Jamieson AM, Diefenbach A, McMahon CW, et al. The role of the NKG2D immunoreceptor in immune cell activation and natural killing. *Immunity* 2002;17:19–29.
- 40 Trapani JA, Smyth MJ. Functional significance of the perforin/granzyme cell death pathway. *Nat Rev Immunol* 2002;2:735–47.
- 41 Huehls AM, Coupet TA, Sentman CL. Bispecific T-cell engagers for cancer immunotherapy. *Immunol Cell Biol* 2015;93:290–6.
- 42 Chan WK, Kang S, Youssef Y, et al. A CS1-NKG2D bispecific antibody collectively activates cytolytic immune cells against multiple myeloma. *Cancer Immunology Research* 2018;6:776–87.
- 43 Voynov V, Adam PJ, Nixon AE, et al. Discovery strategies to maximize the clinical potential of T-cell engaging antibodies for the treatment of solid tumors. *Antibodies* 2020;9. doi:10.3390/antib9040065. [Epub ahead of print: 18 Nov 2020].
- 44 Yano S, Kondo K, Yamaguchi M, et al. Distribution and function of EGFR in human tissue and the effect of EGFR tyrosine kinase inhibition. *Anticancer Res* 2003;23:3639–50.
- 45 Fu X, Meng F, Tao L, et al. A strict-late viral promoter is a strong tumor-specific promoter in the context of an oncolytic herpes simplex virus. *Gene Ther* 2003;10:1458–64.
- 46 Hwang B, Lee JH, Bang D. Single-Cell RNA sequencing technologies and bioinformatics pipelines. *Exp Mol Med* 2018;50:1–14.
- 47 Hedlund E, Deng Q. Single-Cell RNA sequencing: technical advancements and biological applications. *Mol Aspects Med* 2018;59:36–46.
- 48 Du Y, Huang Q, Arisdakessian C, et al. Evaluation of StAR and Kallisto on single cell RNA-Seq data alignment. *G3 Genes[Genetics]* 2020;10:1775–83.
- 49 Liao M, Liu Y, Yuan J, et al. Single-Cell landscape of bronchoalveolar immune cells in patients with COVID-19. *Nat Med* 2020;26:842–4.
- 50 Butler A, Hoffman P, Smibert P, et al. Integrating single-cell transcriptomic data across different conditions, technologies, and species. *Nat Biotechnol* 2018;36:411–20.